ELSEVIER

PHYSICS CONTRIBUTION

A STUDY OF PLANNING DOSE CONSTRAINTS FOR TREATMENT OF NASOPHARYNGEAL CARCINOMA USING A COMMERCIAL INVERSE TREATMENT PLANNING SYSTEM

PING XIA, PH.D., NANCY LEE, M.D., YU-MING LIU, M.D., IAN POON, M.D.,
VIVIAN WEINBERG, PH.D., EDWARD SHIN, M.D., JEANNE M. QUIVEY, M.D., AND
LYNN J. VERHEY, PH.D.

Department of Radiation Oncology, University of California, San Francisco, San Francisco, CA

Purpose: The purpose of this study was to develop and test planning dose constraint templates for tumor and normal structures in the treatment of nasopharyngeal carcinoma (NPC) using a specific commercial inverse treatment planning system.

Methods and Materials: Planning dose constraint templates were developed based on the analyses of dose–volume histograms (DVHs) of tumor targets and adjacent sensitive structures by clinically approved treatment plans of 9 T1–2 and 16 T3–4 NPC patients treated with inverse planned intensity-modulated radiation therapy (IP-IMRT). DVHs of sensitive structures were analyzed by examining multiple defined endpoints, based on the characteristics of each sensitive structure. For each subgroup of patients with T1–2 and T3–4 NPC, the resulting mean values of these defined endpoint doses were considered as templates for planning dose constraints and subsequently applied to a second group of patients, 5 with T1–2 NPC and 5 with T3–4 NPC. The 10 regenerated plans (called new plans) were compared to the original clinical plans that were used to treat the second group of patients, based on plan conformity index and DVHs.

Results: The conformity indices of the new plans were comparable to the original plans with no statistical difference ($p = 0.85$). Among the serial sensitive structures evaluated, there was a significant decrease with the new plans in the dose to the spinal cord when analyzed by the maximum dose ($p = 0.001$), doses encompassing 1 cc of the spinal cord volume ($p = 0.001$) and 3 cc of the spinal cord volume ($p = 0.001$). There was no significant difference in the mean maximum dose to the brainstem between the new plans and the original plans ($p = 0.36$). However, a significant difference in the mean maximum dose to the brainstem was seen among the different T-stages ($p = 0.04$). A decrease with the new plan to the brainstem in the doses encompassing 5% and 10% of the volume was of borderline statistical significance ($p = 0.08$ and $p = 0.06$, respectively). There were no statistical differences between the new plans and the original plans in the mean doses to the chiasm, optic nerve, or eye for each of the endpoints considered. For parallel sensitive structures in the new plans, there was a significant increase in the average mean dose to the parotid glands ($p = 0.01$), a decrease that was of borderline significance in the average mean dose to the temporomandibular joint ($p = 0.07$), but no difference in the average mean dose to the ear.

Conclusions: The statistical analysis showed that new plans are comparable to the original plans for most of the sensitive structures except for a trade-off between a dose reduction to the spinal cord in the new plans and an increase in the mean dose to the parotid glands. These tested planning dose constraint templates can serve as good "starting points" for an inverse plan of NPC using a specific commercial inverse treatment planning system. © 2004 Elsevier Inc.

Intensity-modulated radiotherapy, Head-and-neck cancer, Inverse planning, Optimization.

INTRODUCTION

Radiation therapy is the definitive treatment for nasopharyngeal carcinoma (NPC) [1]. In comparison with the traditional treatment techniques using opposed lateral fields and even with conventional three-dimensional conformal radiotherapy (3D-CRT), inverse-planned (IP) intensity-modulated radiation therapy (IMRT) has been shown to

offer superior dose conformity to the tumor target and better sparing of critical organs in the treatment of NPC (2–10). Unfortunately, the clinical application of IP-IMRT has been hampered by prolonged planning and treatment time. Based on our experience with a specific commercial treatment planning system, the purpose of this study is to develop and test planning dose constraint templates for NPC to achieve better planning efficiency.

In external beam radiotherapy, treatment goals have always aimed at treating the tumor to an adequate dose while protecting the surrounding normal tissues. An appropriate specification of dose constraints for a specific disease site is essential for obtaining an optimal plan that achieves the best compromise between these often conflicting treatment goals. Although facilitated by computer optimization, an IP-IMRT plan is not always optimal if the specification of dose constraints is inappropriate. In most inverse planning systems, the specification of dose constraints is the only input that the operator can control, whereas the formulation of the objective function is often programmed into the planning system. The process of inverse planning becomes time-consuming in that planners must go through much trial and error to adjust the planning dose constraints before an IP-IMRT plan is acceptable for clinical use.

The relationship between the planning dose constraints and the resultant dose distributions is dependent on several factors such as variations in anatomic relationship between the tumor and sensitive structures, special clinical considerations from patient to patient, treatment delivery method, and the characteristics of the inverse planning system. Given this complex relationship, it is often difficult to predict how changes in dose constraints will affect the resultant dose distributions of a treatment plan. It is particularly difficult in the case of NPC because of the complex tumor shape and the large number of adjacent sensitive structures. Despite these difficulties, developing a site-specific planning dose constraint template within an institution using a specific treatment planning system can reduce variations of plan quality among different planners and decrease treatment planning time, because these planning dose constraint templates serve as a good "starting point" for each new plan.

Using their in-house treatment planning system, Hunt *et al.* (11), from Memorial Sloan-Kettering Cancer Center described an IMRT treatment technique using a dynamic multileaf collimator (MLC) with their institutional dose constraint template for NPC. For a specific cancer site, the availability of such dose constraint templates developed from different institutions may stimulate the development of better treatment planning techniques and better treatment outcomes. Such studies will be particularly useful for planners using the same commercial planning systems.

At the University of California-San Francisco, IP-IMRT on NPC was implemented in October 1997. Over the years, our treatment technique has evolved. We initially treated all primary nasopharyngeal tumor with a sequential tomotherapy technique using a special MLC (MIMiC, NOMOS, Sewickley, PA), whereas the regional lymph nodes were treated with conventional fields using a conventional MLC. This technique was then replaced by a technique using multiple fixed gantry angle beams with conventional MLCs (including dynamic MLC from Varian's linear accelerators and static MLC from Siemens linear accelerators) to treat the primary tumor while using conventional fields to treat the regional nodes. Since February 2000, IMRT plans have been used to treat entire target volumes including regional lymph nodes. Excellent treatment outcomes were recently reported for 67 NPC patients treated to date (10).

METHODS AND MATERIALS

Patient selection

Two groups of NPC patients were selected for this study. The first group of patients, consisting of 9 early-stage patients (T1–2) and 16 advanced-stage patients (T3–4) according to the 1997 American Joint Committee on Cancer staging classification, was treated consecutively at our institution with IP-IMRT between October 1997 and January 2000. The dose–volume histograms (DVHs) of the treatment plans were retrospectively analyzed by examining multiple defined endpoints, based on the characteristic of each sensitive structure. For each subgroup of the early-stage and advanced-stage patients, the mean values of the defined endpoint doses, as shown in Tables 1 and 2, were considered as a planning dose constraint template (see "Planning dose constraints" below).

The second group of patients, consisting of 5 early-stage (T1–2) patients and 5 advanced-stage (T3–4) patients, was treated at our institution between February 2000 and December 2002. These patients were selected randomly, and the only criterion is the stage. The stage and tumor extension information for the 10 selected patients is listed in Table 3. By using planning dose constraint templates developed from the first group of patients, new treatment plans were generated and compared to the original clinical plans that were used to treat these patients.

Delineation of target volumes and sensitive structures

All target volumes were outlined slice by slice on the treatment-planning computed tomographic (CT) images, acquired with 3-mm thickness. The gross tumor volume (GTV) was defined as the gross extent of the tumor shown by imaging studies (with use of magnetic resonance imaging and CT images) and included the primary tumor as well as all gross regional lymph nodes. The planning target volume (PTV) was defined by each individual physician to include the margin for potential microscopic spread and uncertainties in delivery. Because the treatment planning system (Corvus, NOMOS, Sewickley, PA) used in our institution does not allow the same region to be defined by two different names, the GTV was excluded from the PTV. The surrounding critical normal structures, namely the brainstem, spinal cord, optic nerves, chiasm, parotid glands,

Table 1. Averaged endpoint doses for the first group of patients with stage T1–2 nasopharyngeal carcinoma

Structures	Max. dose (Gy)	Dose to 5% vol. (Gy)	Dose to 10% vol. (Gy)
Chiasm	27.5 ± 14.1	21.5 ± 9.8	19.7 ± 9.2
Spinal cord*	38.3 ± 9.4	30.6 ± 13.0	25.8 ± 16.6
Brainstem	50.9 ± 3.9	40.4 ± 7.3	37.6 ± 7.2
Optic nerve	23.7 ± 12.1	22.2 ± 11.3	18.8 ± 9.7
Eye	25 ± 15.2	13.5 ± 7.3	9.8 ± 5.0
	Mean dose (Gy)	Dose to 50% vol. (Gy)	Dose to 80% vol. (Gy)
Parotid glands	26.8 ± 4.5	25.1 ± 4.1	17.9 ± 5.1
Temporomandibular joint	33.8 ± 5.0	30.5 ± 5.1	26.7 ± 4.9
Middle/inner ear	41.4 ± 6.0	38.3 ± 10.5	31.3 ± 9.5

* The endpoints are the maximum dose, and doses encompassing 1 cc and 3 cc, respectively.

temporomandibular joints, middle and inner ears, the brain, the tongue, the larynx, and the mandible were also outlined.

Treatment goals and planning criteria

The treatment goal for all NPC patients was to deliver a dose of 70 Gy (2.12 Gy/fraction) to ≥95% of the GTV and a dose of 59.4 Gy (1.8 Gy/fraction) to ≥95% of the PTV simultaneously while keeping doses to all adjacent sensitive structures below tolerance. The tolerance doses to sensitive structures are defined as follows. The maximum point doses to the spinal cord and the brainstem were to be less than 45 Gy and 54 Gy, respectively. However, for some selected cases, the maximum point dose was relaxed to 50 Gy and 60 Gy to the spinal cord and brainstem respectively while keeping the maximum dose encompassing 1 cc of the spinal cord <45 Gy and the maximum dose encompassing 1% of the brainstem <54 Gy. The maximum point doses to the optic structures, such as the chiasm and optic nerves, were to be less than 54 Gy. The mean dose to either parotid gland was to be less than 26 Gy. The maximum point doses to the temporomandibular joints and mandible were to be less than 70 Gy (or no more than 1 cc of the volume received a dose >70 Gy). The doses to other structures such as the middle and inner ears, brain, tongue, and larynx were intended to be as low as possible.

Planning dose constraints

The planning dose constraints were developed on the basis of a retrospective analysis of treatment plans for the first group of patients. Briefly, all plans were normalized to an isodose line such that more than 95% of the GTV received a dose of 70 Gy whereas more than 95% of the PTV received a dose of 59.4 Gy. DVHs of all sensitive structures were characterized by multiple endpoints, depending on the functional subunit organization in each structure. There are many ways to choose endpoints in characterizing a DVH curve. For serial sensitive structures, the maximum point dose is an interesting endpoint, yet this endpoint depends on the dose calculation resolution and the dose algorithm. To reflect the characteristics of DVHs in high dose regions for serial structures including the brainstem, optic chiasm, optic nerves, and eyes, we chose two additional endpoints such as the dose encompassing 5% and 10% of the sensitive structure volume. For the spinal cord, volumes of 1 cc and 3 cc of the involved spinal cord were used because the contour does not include the entire spinal cord (from cervical to lumbar region). For sensitive structures with functional subunit in parallel such as the parotid glands, the temporomandibular joints, and the inner and middle ear, the mean dose and the doses encompassing 50% and 80% of the volumes were chosen as endpoints. For

Table 2. Averaged endpoint doses for the first group of patients with stage T3–4 nasopharyngeal carcinoma

Structures	Mean dose (Gy)	Dose to 5% vol. (Gy)	Dose to 10% vol. (Gy)
Chiasm	42.7 ± 10.2	36.4 ± 11.0	34.2 ± 9.4
Spinal cord*	42.2 ± 10.4	33.0 ± 12.8	26.7 ± 17.3
Brainstem	55.3 ± 6.7	43.1 ± 8.7	40.0 ± 9.8
Optic nerve	41.6 ± 14.5	34.4 ± 13.0	31.6 ± 13.4
Eye	32.8 ± 15.4	21.9 ± 13.3	19.6 ± 12.3
	Max. dose (Gy)	Dose to 50% vol. (Gy)	Dose to 80% vol. (Gy)
Parotid glands	27.8 ± 6.0	24.6 ± 5.9	18.7 ± 6.2
Temporomandibular joint	38 ± 6.4	36.7 ± 7.4	31.5 ± 5.8
Middle/inner ear	49.6 ± 12.0	49.8 ± 12.4	42.2 ± 12.4

* The endpoints are the maximum dose, and doses encompassing 1 cc and 3 cc, respectively.

Table 3. Stage and tumor extension information about 10 selected patients

Patient	Stage	Tumor extension	Patient	Stage	Tumor extension
A1	T1N0	Right	B1	T3N0	Right
A2	T1N0	Right	B2	T3N2	Left
A3	T2N1	Right	B3	T3N2	Central
A4	T2N0	Central	B4	T4	Right
A5	T2N2	Central	B5	T4	Right

these defined endpoints, the planning dose constraints used for the second group of patients, as shown in Tables 1 and 2, were the mean endpoint doses obtained from the first group of patients for early and advanced stages separately. As mentioned previously, there were other contoured sensitive structures, such as the tongue, mandible, larynx, and brain, but due to large inconsistencies in contouring these structures, DVH evaluation of these structures was omitted from this analysis.

Planning system

A commercial inverse planning system (Corvus, NO-MOS) has been used in our clinic since 1997. Treatment plans for the first group of patients were generated with several software versions (Peacock 1.2, Corvus 2.0, Corvus 3.0). The original plans and regenerated plans for the second group of patients were generated with Corvus version 4.0. In the Corvus system, dose constraints for each structure can be depicted as a simplified three-point DVH, namely a dose goal or limit, a minimum dose, and a maximum dose. Figure 1 shows the input dose constraints for the GTV, PTV, and selected sensitive structures involved for a T2 NPC case. Note that Fig. 1 does not include all input dose constraints used in the treatment planning process. The partial volume effect was reflected by the parameter of "volume below goal" for the targets or "volume above limit" for sensitive

structures. It should be noted that the number of endpoints (see Tables 1 and 2) defined in the analysis of DVHs for the first group of patient was more than the number of dose constraint parameters required for the Corvus planning system. For each serial structure, the average value of the dose encompassing 5% of the volume was used as the dose limit. For each parallel structure, the average dose encompassing 50% of the volume was used as the dose limit. The minimum doses to all sensitive structures were not critical, and thus remained the same as in the original plan.

In addition to these dose–volume parameters, there are other parameters in the Corvus system which can affect the quality of a plan, such as the "importance" (if checked in column I in Fig. 1) and choice of the "type" of the structure. For example, a biologically uniform structure (labeled as BU structure in Fig. 1) is used for a parallel structure. These parameters reflect the characteristics of a structure, which determine the penalty factor if the dose–volume parameters are violated. In the regenerated plans, these parameters were kept the same as in the original plans.

Treatment techniques

As mentioned earlier, in our institution IMRT treatment techniques have evolved but the treatment goals have remained the same, particularly for the tumor volumes and the prescribed doses. The treatment techniques used for the first

Target Name	Type		Goal (Gy)	Vol Below Goal (%)	Min (Gy)	Max (Gy)	I
GTV - target	■	Basic	70.0	5	60.0	77.0	
CTV1 - target	■	Basic	59.4	5	54.0	70.0	

Sensitive Structure Name	Type		Limit (Gy)	Vol Above Limit (%)	Min (Gy)	Max (Gy)	I
Tissue	■	Basic Tissue	54.0	0	0.0	59.4	
Spinal cord	□	Basic Structure	38.3	1	15.0	45.0	
LT-Parotid	□	BU Structure	24.0	30	15.0	60.0	
RT-Parotid	□	BU Structure	24.0	30	15.0	60.0	
Brain-Stem	□	Basic Structure	50.0	1	20.0	52.0	

Fig. 1. The selected input dose–volume constraints from a commercial treatment planning system for a typical T2 stage nasopharyngeal case.
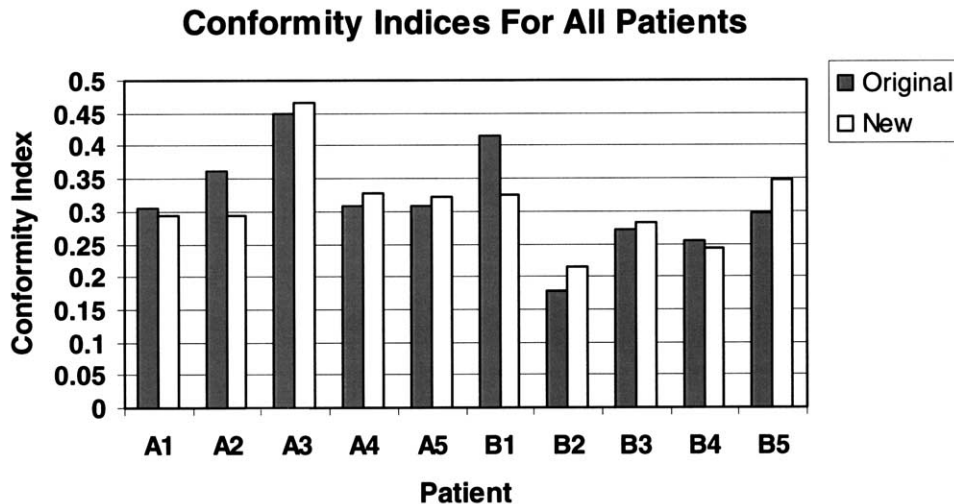
Conformity Indices For All Patients

Fig. 2. The dose conformity indices (COIN) of the original plans and regenerated plans for 5 T1–2 and 5 T3–4 cases.

group of patients employed either a MIMIC delivery with 5 to 7 arcs of 270° using 1 cm mode and 10 intensity levels, or a step-and-shoot MLC delivery with 9 to 15 fixed gantry angles and 5 to 10 nonzero intensity levels. At the discretion of the radiation oncologist, the upper neck nodes and the supraclavicular nodes were treated by one of three options: (*1*) with a conventional technique; (*2*) the upper neck nodes were treated with the IMRT fields and the supraclavicular nodes were treated with a conventional anterior field; (*3*) the entire neck node regions were treated with the IMRT fields. The treatment planning details were reported previously (12).

As our experience increased, the variation in treatment technique for the second group of patients was smaller than that for the first group of patients. The number of gantry angles used in each plan was reduced to 8 or 9 beam angles while keeping the plan acceptance criteria the same. All plans from the second group of patients used 6-MV photon beams (Siemens linear accelerators) with five nonzero intensity levels and delivered with static MLCs. The delivery method for the regenerated plans, including beam directions and beam energy, remained the same as in the original plans. The only changes made were the planning dose constraints.

Plan evaluation

For the second group of patients including 5 T1–2 and 5 T3–4 stage patients, 10 clinical plans and 10 regenerated plans were evaluated. For simplicity, we refer to the clinically approved plan as the "original" plan and the regenerated plan as the "new" plan. All plans were normalized such that an isodose line of 70 Gy should cover ≥95% of the GTV while the 59.4 Gy isodose line should cover ≥95% of the PTV simultaneously. The original plan and the new plan were compared using the defined multiple endpoint doses as listed in Tables 2 and 3, as well as the dose conformity

index (COIN). The dose conformity index was based on the definition of COIN proposed by Baltas *et al.* (13), as shown in the following equation:

$$COIN = c_1 \times c_2.$$

$$\text{Where} \quad c_1 = \frac{PTV_{ref}}{PTV},$$

$$c_2 = \frac{PTV_{ref}}{V_{ref}}, \quad (1)$$

The PTV volume used for this equation included the GTV volume, whereas the PTV used elsewhere in this study excluded the GTV volume. The PTV_{ref} is the fraction of the PTV that is enclosed by the prescribed isodose line of 59.4 Gy, and the V_{ref} is the tissue volume that is enclosed by the prescribed isodose line. The ideal situation is for both c_1 and c_2 to be equal to 1.

Descriptive statistics (e.g., mean, standard deviation) were calculated to characterize the dose for each plan by stage and structure. Analysis of variance methods for repeated measures were used to analyze the change in mean values when the new constraints were applied to the original treatment plans. For some structures there was a planned difference between the two subsets in the constraint that was applied (e.g., maximum dose to the chiasm) and statistical differences in mean values would be anticipated. Therefore, T stage was included as a main factor in the analysis of variance model to account for this difference. In addition, when dosing for both left and right sides for structures was available, this was also included as a repeated measure in the model.

RESULTS

Plan conformity and homogeneity

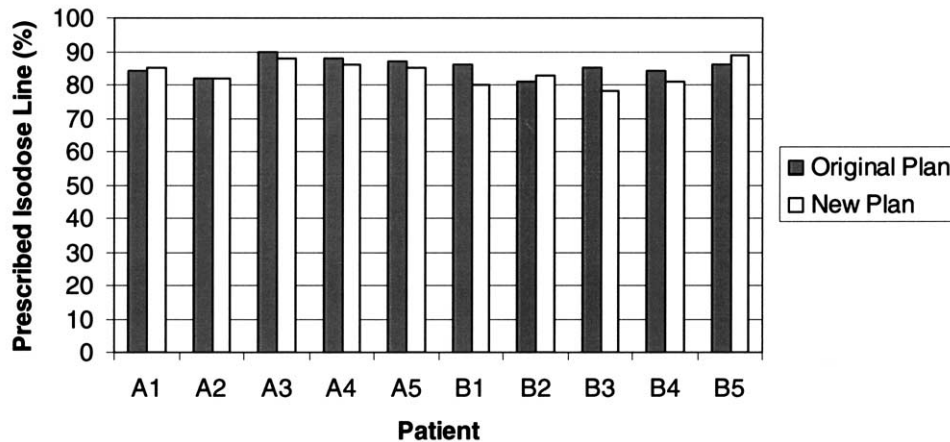Figure 2 shows the conformity indices of the original and

Fig. 3. The prescribed isodose lines (in percentage of the maximum dose of each plan), reflecting dose homogeneity inside the tumor volume.

new plans for the second group of patients, with an ideal conformity index being equal to 1. Among all patients, conformity indices of the new plans were comparable to the original plans with no statistical difference ($p = 0.85$). Figure 3 shows the prescribed isodose lines (in percentage of the maximum dose of each plan), reflecting dose homogeneity inside the GTV since these prescribed isodose lines were normalized to a dose of 70 Gy. In each plan, the prescribed isodose line was selected such that it covered ≥95% of the GTV while the 59.4 Gy isodose line covered ≥95% of the PTV simultaneously. The ranges of the prescribed isodose lines were 81–90%, and 78–89%, with the average prescribed isodose lines of 85.3 ± 2.6%, 83.7 ± 3.3% for the original and new plans, respectively.

Serial structures

Among the serial-sensitive structures evaluated, there was a significant decrease with the new plans in the dose delivered to the spinal cord when analyzed by the maximum dose ($p = 0.001$), doses encompassing 1 cc of the volume ($p = 0.001$) and 3 cc of the volume ($p = 0.001$). No difference was seen in these endpoint doses of the spinal cord due to different T-stages. For the mean maximum dose delivered to the brainstem, there was no difference between the new plans and the original plans ($p = 0.36$), but a significant difference due to T-stage was observed with T3–4 patients receiving higher doses to the brainstem ($p = 0.04$). For the doses encompassing 5% and 10% of the brainstem volume, a decrease with the new plan was of borderline statistical significance ($p = 0.08$ and $p = 0.06$, respectively). There were no statistical differences between the new plans and the original plans in the mean endpoint doses (the maximum dose, the doses encompassing 5% and 10% of the volume) to the chiasm, optic nerve, or eye for each of the endpoints considered. Because of less cranial involvement for patients with early-stage disease, stage T1–2 patients received significantly lower doses to the chiasm compared to stage

T3–4 patients when analyzed by the maximum dose ($p = 0.03$), dose encompassing 5% of volume ($p = 0.02$) and 10% of the volume ($p = 0.02$).

The details of the comparison of average endpoint doses for selected serial structure are shown in Tables 4 and 5. It was observed for T1–2 patients that the average maximum point dose of the spinal cord was reduced from 45.3 ± 2.4 Gy in the original plans to 37.2 ± 3.9 Gy in the new plans. Similarly, the average maximum point dose of the brainstem was reduced from 54.8 ± 2.7 Gy in the original plans to 51.1 ± 1.5 Gy in the new plans. Although the average maximum point doses from the original plans almost met our dose limits of 45 Gy for the spinal cord and 54 Gy for the brainstem, this exercise indicated that we would be able to reduce these maximum doses further. For T3–4 patients, a comparable decrease with the new plan was observed in the mean maximum dose to the spinal cord (45.6 ± 2.3 Gy reduced to 41.2 ± 4.1 Gy) but not to the brainstem (57.7 ± 2.8 Gy increased to 59.0 ± 6.8 Gy). Although the average maximum point dose of the brainstem was increased in new plans, the average dose encompassing 5% of the brainstem was reduced from 48.6 ± 3.0 Gy in the original plans to 47.6 ± 6.8 Gy in the new plans. Depending on the plan acceptance criteria established by each institution, the dose constraints to the maximum doses of the brainstem in some new plans may require further adjustments. Although there is a dose reduction to the spinal cord with the new plans, there has been a corresponding increase of the average mean dose to the parotid gland, as discussed below.

For T1–2 patients, Fig. 4a displays the selected endpoint doses of serial structures from the original plans and the new plans as a percent of the planning constraints. The 100% line indicates when the dose equaled the planning dose constraint. As shown in Fig. 4a, the endpoints for each sensitive structure from the new plans are clustered around the 100% line, resulting in smaller variations from the planning dose constraint than that of the original plans. Greater variability in endpoint doses to the chiasm was

Table 4. Comparison of selected average endpoint doses for sensitive structures in T1–2 NPC patients

Structure	Endpoint	Planning dose constraint (Gy)	Endpoint dose in original plan (Gy)	Endpoint dose in new plan (Gy)
Serial structures				
Chiasm	max dose	27.5	36.5 ± 14.6	30.0 ± 6.1
	to 5% V	21.5	30.9 ± 13.8	24.0 ± 6.0
Spinal cord	max dose	38.3	45.3 ± 2.4	37.2 ± 3.9
	to 1 mL V	30.6	38.5 ± 2.9	30.1 ± 2.3
Brainstem	max dose	50.9	54.8 ± 2.7	51.1 ± 1.5
	to 5% V	40.4	47.7 ± 2.2	41.8 ± 3.3
Left optic nerve	max dose	23.7	20.7 ± 12.2	23.6 ± 7.3
	to 5% V	22.2	17.4 ± 10.8	18.9 ± 8.9
Left eye	max dose	25.0	32.6 ± 12.5	23.9 ± 5.6
	to 5% V	13.5	23.4 ± 13.2	14.6 ± 2.9
Parallel structures				
Left parotid	mean dose	26.8	28.4 ± 1.1	30.9 ± 1.3
	to 50% V	25.1	25.2 ± 2.5	25.2 ± 1.8
Left TMJ	mean dose	33.8	34.8 ± 10.8	29.4 ± 5.2
	to 50% V	30.5	34.9 ± 11.9	28.4 ± 5.0
Left ear	mean dose	41.4	35.7 ± 9.8	33.7 ± 11.8
	to 50% V	38.3	35.6 ± 10.7	33.8 ± 13.1

Abbreviations: NPC = nasopharyngeal carcinoma; TMJ = temporomandibular joint; V = volume.

observed as a result of different cranial involvement for early-stage patients, indicating that the planning dose constraint to the chiasm might require further individual adjustment to obtain an optimal plan.

Similarly, Fig. 4b displays the selected endpoint doses of serial structures for T3–4 patients, comparing the original plans with the new plans as a percentage of the planning constraints. In comparison with T1–2 patients, variations among the endpoint doses evaluated were smaller for both new plans and the original plans. The endpoint doses with

the new plans were slightly closer to the planning dose constraints.

Parallel structures

In comparison between the new plans and the original plans for parallel sensitive structures, there was a significant increase in the average mean dose delivered to the parotid glands ($p = 0.01$). However, there is no significant change in the average dose to 50% of the parotid volume ($p = 0.18$). There was also a decrease in the average mean dose

Table 5. Comparison of selected averaged endpoint doses for sensitive structures in T3–4 NPC patients

Structure	Endpoint	Planning dose constraint (Gy)	Endpoint dose in original plan (Gy)	Endpoint dose in new plan (Gy)
Serial structures				
Chiasm	max dose	42.7	46.7 ± 6.1	46.5 ± 4.3
	to 5% V	36.4	41.0 ± 4.4	39.3 ± 1.6
Spinal cord	max dose	42.2	45.6 ± 2.3	41.2 ± 4.1
	to 1 ml V	33.0	38.6 ± 2.1	33.4 ± 4.5
Brainstem	max dose	55.3	57.7 ± 2.9	59.0 ± 6.8
	To 5% V	43.1	48.6 ± 3.0	47.6 ± 6.5
Left optic nerve	max dose	41.6	39.9 ± 16.3	38.8 ± 13.3
	to 5% V	34.4	35.5 ± 15.7	33.1 ± 11.5
Left eye	max dose	32.8	39.3 ± 13.1	35.8 ± 13.5
	to 5% V	21.9	25.3 ± 11.7	22.9 ± 10.3
Parallel structures				
Left parotid	mean dose	27.8	27.1 ± 4.1	30.9 ± 2.8
	to 50% V	24.6	24.9 ± 3.9	27.3 ± 2.7
Left TMJ	mean dose	38.0	43.3 ± 5.1	39.0 ± 7.3
	to 50% V	36.7	42.9 ± 6.6	37.3 ± 7.7
Left ear	mean dose	49.6	38.2 ± 7.2	41.0 ± 6.2
	to 50% V	49.8	37.6 ± 7.7	40.5 ± 6.0

Abbreviations as in Table 1.

T1-2 Patients
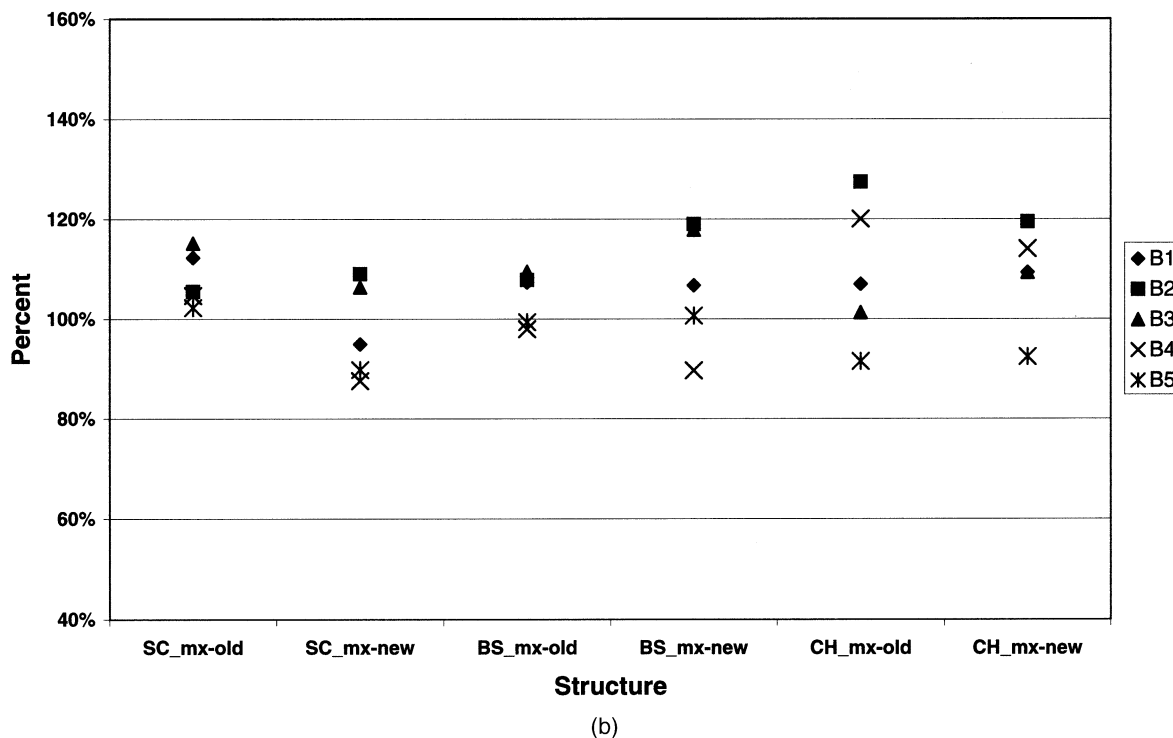

(a)

T3-4 Patients

(b)
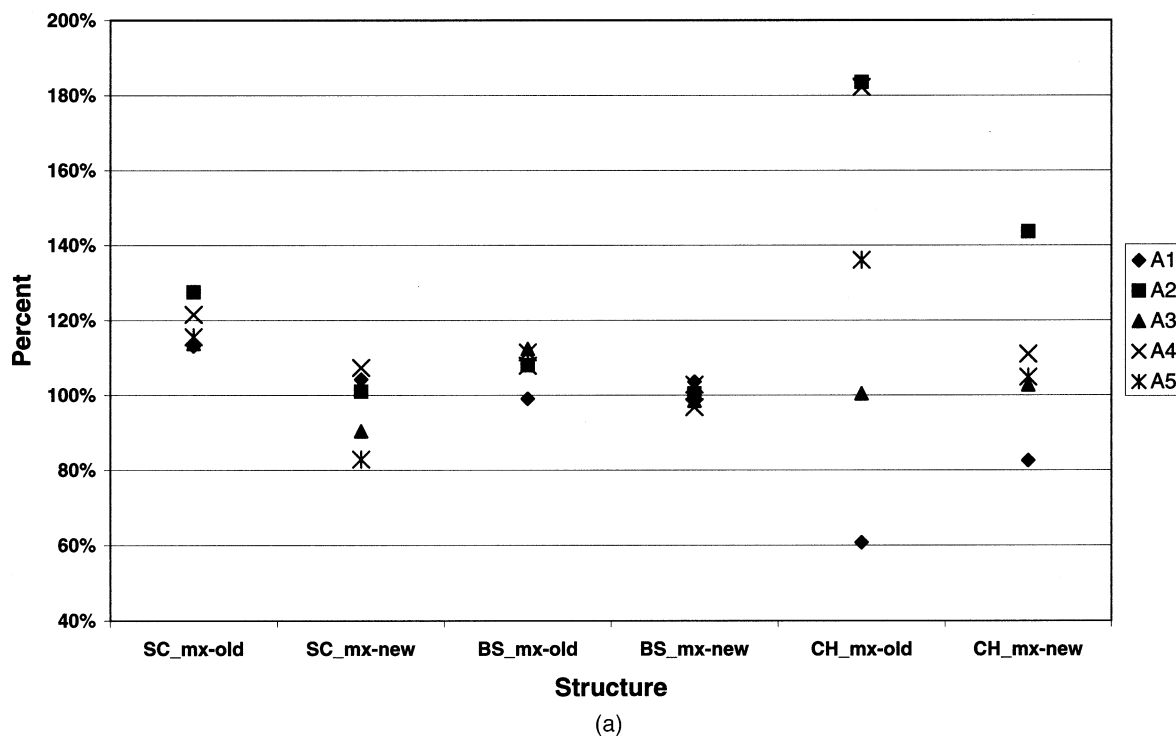
Fig. 4. The selected endpoint doses of serial structures from the original plans and the new plans are displayed as a percent of the planning constraints. The 100% line indicates when the dose equaled the planning dose constraint. (a) T1–2 patients, (b) T3–4 patients. "Old" means the original plans, "new" means the new plans. SC_mx = maximum point dose to the spinal cord; BS_mx = maximum point dose to the brainstem; CH_mx = maximum point dose to chiasm.

to the temporomandibular joints of borderline significance ($p = 0.07$), but no difference in the average mean dose to the inner/middle ears. There was a borderline difference in the average mean dose to the ears due to T-stage with the T3–4 patients receiving higher mean doses to the ears. This difference was also anticipated based upon the planning dose constraints, as shown in Tables 4 and 5. There was no difference due to side (right vs. left) for any of these structures.

The increased average mean dose to the parotid glands noted above in the new plans for both subgroups indicates that the dose reduction to the spinal cord in the new plans is "traded off" with the increase of the mean dose to the parotid gland. In our current practice, the planning dose constraint has been further reduced to allow 30% of the parotid volume to exceed 24 Gy while keeping the same dose constraint to the spinal cord.

Figures 5a and 5b display the selected endpoint doses of parallel structures from the original and new plans as a percent of the planning dose constraints for T1–2 patients and T3–4 patients, respectively. Because there was no difference due to left or right side of the organ for these parallel structures, only right side organs were shown in Fig. 5a and Fig. 5b. The 100% line indicates when the endpoint dose equaled the planning dose constraint. For T3–4 patients, for all parallel structures as shown in Figs. 5a and 5b, the endpoint dose variations among all patients were comparable between the new and the original plans.

DISCUSSION

The planning dose constraint templates for NPC used in this study are from a single institution, using a specific commercial treatment planning system. These dose constraints cannot and should not be directly applied to other treatment planning systems that employ different optimization schemes. Development of planning dose constraint templates for a specific treatment site evolves as technologies in treatment planning and delivery improve, and as the experience of those using these technologies increases. Despite improvement in technology and increased experience in the application of these technologies, this study indicates that periodic reevaluation of the planning dose constraint templates for the surrounding normal tissue may provide valuable information that can lead to standardization of the planning process. For example, the planning dose constraint templates in this study were based on the mean endpoint doses from the DVHs of 25 NPC patients previously treated with a variety of treatment technologies, yet using the planning dose constraint templates in the new plans for the second group of patients achieved comparable plan quality without adjustment of planning dose constraints. Because of variations in the anatomic relationships between the tumor and sensitive structures and because of special patient-specific clinical considerations, the planning dose constraint templates can be used only as a good "starting point," and patient-specific adjustments should be applied as needed to account for these clinical variations. The use of planning dose constraint templates improves planning efficiency, with significant reduction in the number of adjustments in dose constraints in the subsequent planning process. In our practice, we have reduced the scheduled planning time from 1 week to 2 days once the tumor volumes are contoured. The average planning time for an NPC case is about 4–8 h, including contouring time for all surrounding sensitive structures.

The comparison made between the new plans and the original plans may be biased in favor of new plans, because for each sensitive structure one of the defined endpoints was used as a planning dose constraint in the new plans, whereas dose constraints used in the original plans were not based on the planning dose constraint templates. On the other hand, for each sensitive structure, three defined endpoints were used for plan comparison whereas only one endpoint was used as an input planning dose constraint. All new plans might not be clinically accepted because comparison of endpoint doses is not sufficient for acceptance of a clinical plan. However, this exercise provides guidelines for achievable endpoints. For a plan to be clinically accepted, detailed isodose distributions, especially the locations of hot spots and cold spots, must be carefully examined, and additional adjustments made if required.

The planning dose constraint templates reported in this study are based on a specific inverse planning system. In particular, this system allows each voxel to be identified with only one structure. For example, the PTV defined by this system excludes the GTV, whereas in other treatment planning systems, the PTV may include the GTV. Similarly, if the PTV overlaps other sensitive structures, the volume of these sensitive structures may not be accurate and the maximum dose points to the sensitive structure may not be indicated on the DVH. In the case of NPC, the parotid gland may overlap the PTV. In our institution, if there is a significant overlap region between the PTV and the parotid glands, another plan with corrected parotid gland contours (called a phantom plan) will be recalculated using the same beam configurations (including intensity patterns) as in the clinically approved plan, to obtain a correct DVH for the parotid glands.

CONCLUSIONS

Efficient inverse planning in IMRT requires *a priori* knowledge about dose–volume constraints on the surrounding sensitive structures, which can be obtained from the DVHs of previous clinical treatment plans. Using the mean DVHs of these plans and our specific inverse treatment planning system, we have developed two sets of planning dose constraint templates for early- and late-stage NPC, providing an excellent tool for improved efficiency in treatment planning. The statistical analysis shows that new plans are comparable to the original plans for most sensitive structures. Physicians may decide to adjust dose constraints based on their

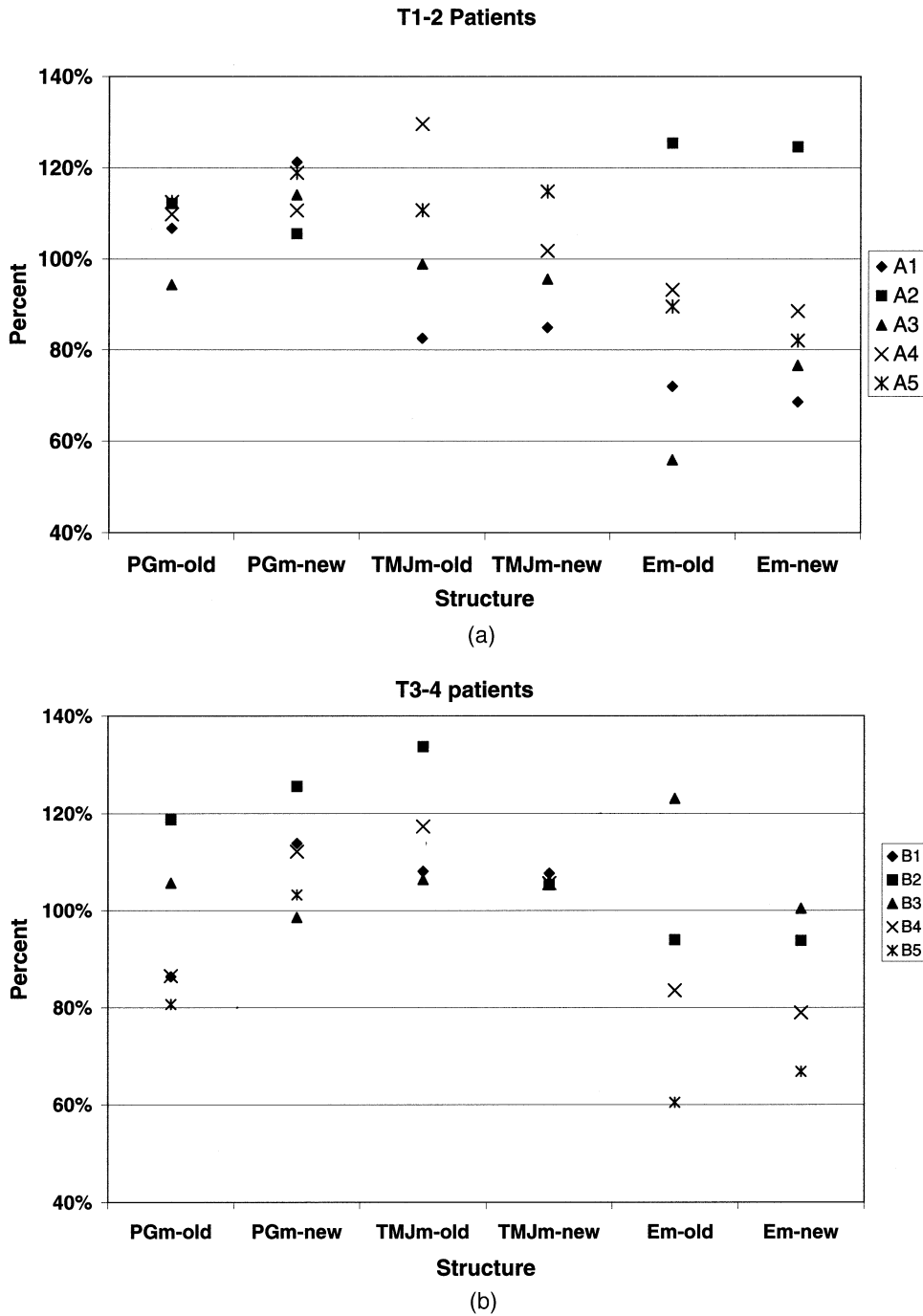**T1-2 Patients**

(a)

T3-4 patients

(b)

Fig. 5. The selected endpoint doses of right side parallel structures from the original and new plans are displayed as a percent of the planning dose constraints. The 100% line indicates when the endpoint dose equaled the planning dose constraint. (a) T1–2 patients, and (b) T3–4 patients. "Old" means the original plans, "new" means the new plans. PGm = mean dose to the right parotid gland volume; TMJm = mean dose to the right temporomandibular joint; Em = mean dose to the right ear.

clinical judgment for individual cases. The tested planning dose constraint templates, however, can serve as a

good "starting point" for an inverse plan of NPC using a specific commercial inverse treatment planning system.

REFERENCES

1. Marks JE, Bedwinek JM, Lee F, Purdy JA, Perez CA. Dose-response analysis for nasopharyngeal carcinoma: An historical perspective. *Cancer* 1982;50:1042–1050.

2. Leibel SA, Kutcher GJ, Harrison LB, *et al.* Improved dose distributions for 3D conformal boost treatments in carcinoma of the nasopharynx. *Int J Radiat Oncol Biol Phys* 1991;20:823–833.

3. Kutcher GJ, Fuks Z, Brenner H, *et al.* Three-dimensional photon treatment planning for carcinoma of the nasopharynx. *Int J Radiat Oncol Biol Phys* 1991;21:169–182.

4. Eisbruch A, Marsh LH, Martel MK, *et al.* Comprehensive irradiation of head and neck cancer using conformal multisegmental fields: Assessment of target coverage and noninvolved tissue sparing. *Int J Radiat Oncol Biol Phys* 1998;41:559–568.

5. Sultanem K, Shu HK, Xia P, *et al.* Three-dimensional intensity-modulated radiotherapy in the treatment of nasopharyngeal carcinoma: The University of California-San Francisco experience. *Int J Radiat Oncol Biol Phys* 2000;48:711–722.

6. Wu Q, Manning M, Schmidt-Ullrich R, *et al.* The potential for sparing of parotids and escalation of biological effective dose with intensity modulated radiation treatment of head and neck cancer: A treatment design study. *Int J Radiat Oncol Biol Phys* 2000;46:195–205.

7. Verellen D, Linthout N, van den Berge D, Bel A, Storme G. Initial experience with intensity-modulated conformal radiation therapy for treatment of the head and neck region. *Int J Radiat Oncol Biol Phys* 1997;39:99–114.

8. Chao K, Low D, Perez C, *et al.* Intensity-modulated radiation therapy in head and neck cancer: The Mallinckrodt experience. *Int J Cancer (Radiat Oncol Invest)* 2000;90:92–103.

9. Kuppersmith RB, Greco SC, Teh BS, *et al.* Intensity-modulated radiotherapy: First results with this new technology on neoplasms of the head and neck. *Ear Nose Throat J* 1999;78: 238, 241–246, 248 passim.

10. Lee N, Xia P, Quivey J, *et al.* Intensity-modulated radiotherapy in the treatment of nasopharyngeal carcinoma: An update of the UCSF experience. *Int J Radiat Oncol Biol Phys* 2002; 53:12–22.

11. Hunt MA, Zelefsky MJ, Wolden S, *et al.* Treatment planning and delivery of intensity-modulated radiation therapy for primary nasopharynx cancer. *Int J Radiat Oncol Biol Phys* 2001; 49:623–632.

12. Xia P, Fu KK, Wong G, Akazawa C, Verhey LJ. Comparison of treatment plans involving intensity-modulated radiotherapy for nasopharyngeal carcinoma. *Int J Radiat Oncol Biol Phys* 2000;48:329–337.

13. Baltas D, Kolotas C, Geramani K, *et al.* A conformal index (COIN) to evaluate implant quality and dose specification in brachytherapy. *Int J Radiat Oncol Biol Phys* 1998;40:515–524.